Pressureless nanoimprinting of anatase TiO_2 precursor films

Dustin A. Richmond
Washington Technology Center, Seattle, Washington 98195 and Department of Electrical Engineering, University of Washington, Campus Box 352500, Seattle, Washington 98195

Qifeng Zhang and Guozhong Cao
Department of Materials Science and Engineering, University of Washington, Campus Box 352120, Seattle, Washington 98195

Dirk N. Weiss[a)]
Washington Technology Center, Seattle, Washington 98195 and Department of Electrical Engineering, University of Washington, Campus Box 352500, Seattle, Washington 98195

(Received 2 December 2010; accepted 13 February 2011; published 14 March 2011)

A soft-imprint method for obtaining anatase TiO_2 nanostructures is reported. The method is *de facto* pressureless and is performed without the need for dedicated imprint equipment. A titanium butoxide-based sol precursor is prepared with a heavy alcohol, methoxy ethanol, as a solvent. The use of an incompletely cross-linked very soft polydimethylsiloxane mold is found to be crucial for obtaining large-area high-quality imprints. The authors discuss quantitatively the observed substrate-constrained shrinkage of pillars and lines (ridges) during annealing. © *2011 American Vacuum Society.* [DOI: 10.1116/1.3562955]

I. INTRODUCTION

Thermal embossing or nanoimprinting of ceramic precursor materials has attracted the interest of researchers and technologists for several decades[1–19] because of the inherent advantages of *directly* nanopatterning and micropatterning functional films without additional steps of ion etching and lithography-resist removal.[18] In photonics applications, for example, nanoscale patterning allows for the control of light propagation through thin-film structures. Titanium dioxide (TiO_2) is, in this regard, a particularly attractive material because of its transparency and high index of refraction.[10,11,16] One such example from the literature is a patterned matrix for distributed-feedback quantum-dot lasers;[10] another proposed use is as dielectric cladding for diffractive back reflectors for thin-film solar cells.[19] Other applications may include waveguides with integrated grating couplers, photocatalytic surfaces, and sensing devices.[11] Sundar *et al.* successfully patterned TiO_2 prepolymer films prepared with an ethanolic solution of titanium butoxide ($Ti(OBu)_4$) by embossing with an elastomeric polydimethylsiloxane (PDMS) mold.[10] A similar chemistry was recently employed by Yoon *et al.*, who demonstrated the patterning of small pillars.[16] This previous work, however, had the disadvantage of requiring pressure during imprinting, which in the case of soft PDMS molds can easily distort mold features. Also, the inherent shrinkage of sol-based precursor materials led to pattern features with relatively small aspect ratios.[16] Here, we present a significantly improved method that employs *de facto* pressureless nanoimprinting with very soft PDMS molds and partially hydrolyzed prepolymer precursor films. This method is enabled by the use of a heavy alcohol as precursor solvent, which produces homogeneously thick yet sufficiently compliant films, and the use of partially heat-cured PDMS imprint molds, which afford the application of negligible pressure during imprinting, thus avoiding distortion of the PDMS mold features. We demonstrate areas up to 5.5 cm^2 that are imprinted approximately 80% without major defects. Volumetric material shrinkage causes height shrinkage for the pillar structures of 56%—a smaller degree of shrinkage than reported in the literature for a comparable precursor material (68% shrinkage).[16] The annealed film material is identified through x-ray diffraction (XRD) as anatase TiO_2. The optical constants are characterized by ellipsometry, which reveals very low absorption and an index of refraction of only less than 10% smaller than that of the dense bulk material.

II. EXPERIMENT

A. TiO_2 precursor solution

The 1*M* TiO_2 precursor solution is prepared following the recipe published by Yoon *et al.*,[16] with two important changes: both $Ti(OBu)_4$ and amine concentrations are doubled and ethanol is substituted for a heavier alcohol, 2-methoxyethanol. First, 6.81 ml of $Ti(OBu)_4$ (97%, Aldrich) is mixed with 1.92 ml of diethanolamine (99%, Sigma-Aldrich) and 9.09 ml of 2-methoxyethanol (JT-Baker) in a dry box with a relative humidity $<30\%$. The solution is then stirred in a capped vial for 2 h at room temperature. Finally, a mixture of 0.18 ml of de-ionized water and 2 ml of 2-methoxyethanol is added to the first solution dropwise while stirring. This solution can last up to 2 weeks without significant precipitation.

B. PDMS mold

We use soft PDMS imprint molds, fabricated by casting against a silicon master mold.[18,20] The master molds were

[a)]Electronic mail: dnweiss@uw.edu

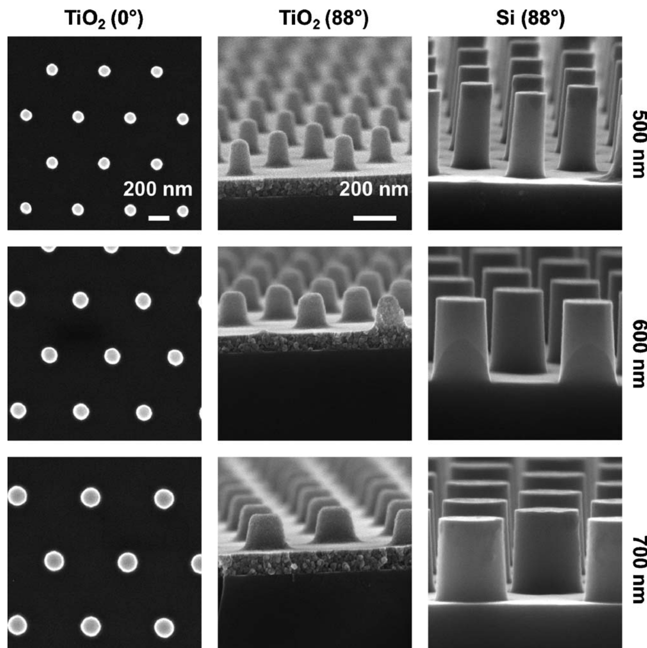

FIG. 1. SEM micrographs of nanoimprinted TiO_2 pillar arrays and corresponding Si master molds, as labeled, for three different patterns defined by the grating periods: 500, 600, and 700 nm. All 0° and all 88° images have the same respective magnifications.

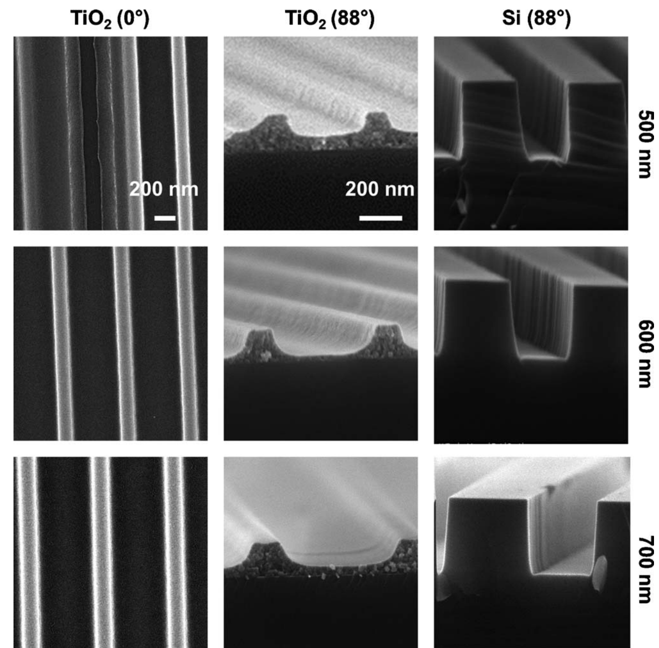

FIG. 2. SEM micrographs of nanoimprinted TiO_2 line gratings and corresponding Si master molds, as labeled, for three different line gratings, defined by the grating periods: 500, 600, and 700 nm. All 0° and all 88° images have the same respective magnifications.

custom fabricated by Lightsmyth Technologies and consist of nine fields, each 8×8 mm^2 large and each with a different pattern: hexagonal pillar arrays, square pillar arrays, and line gratings, each with periods of 500, 600, and 700 nm. The periods chosen are well matched to solar-photonic applications.[19] Laser applications for visible light require slightly smaller periods (300–350 nm range),[10] but we believe our method is easily extendable to this range. The surface of the silicon master mold is first functionalized with fluorosilane using standard methods.[18] The silicon mold is then placed pattern up in an aluminum foil dish and covered with PDMS (Sylgard 184, Dow Corning Corporation, Midland, MI, 1:10 curing agent to prepolymer weight ratio). After degassing in a vacuum desiccator for 30 min, the foil dish is placed in an oven at 80 °C for 30 min to cross-link the PDMS. The material is deliberately cured at lower temperature and for a shorter duration than the 100 °C and 45 min recommended by Dow Corning in order to obtain a markedly softer material. Then the foil is peeled from the PDMS, the Si mold is carefully cut away using a razor blade, and all of the excess PDMS surrounding the mold is removed. The PDMS molds are used for imprinting within 2 h after curing to prevent further hardening of the PDMS.

C. Nanoimprint routine and annealing

A silicon-wafer substrate is first plasma cleaned as described earlier.[18] 1 ml of TiO_2 precursor solution is deposited through a syringe filter (Whatman, polytetrafluoroethylene, 0.45 μm pore size) onto the substrate and spin coated at 6000 rpm for 1 s with an acceleration of 9000 rpm/s. The spin speed is then decelerated to 0 rpm within 1.5 s. The relatively short duration of spin coating allows for an adequate amount of solvent to remain in the precursor film, yet it is sufficiently long to produce a very homogeneous film thickness. Immediately after the substrate stops spinning, the PDMS mold is pressed to the wafer surface by hand with gentle, even pressure, which is applied for about 1 s. With the PDMS mold sticking to the film, the substrate is placed to an annealing furnace and heated for 10 min at 100 °C in air. The PDMS mold is carefully peeled off the film, revealing a strong diffraction grating visible to the eye. The film is then annealed for 15 min at 400 °C in air with a slow temperature ramp of 10 °C/min. To remove any remaining organic material, the film is finally annealed for 1 h at 500 °C in air (80 °C/min temperature ramp).

D. Characterization methods

Imprint and Si master topographies are imaged with scanning-electron microscopy (SEM) using an FEI Sirion microscope with 5 kV acceleration voltage and through-lens detector. 5-nm-thick AuPd alloy films are sputter coated onto TiO_2 samples prior to SEM imaging. XRD is performed in θ-2θ geometry using a Bruker F8 focus powder XRD tool, operating with Cu $K\alpha$ radiation. Optical film constants are measured with a Woollam M-2000 spectroscopic ellipsometer.

III. RESULTS AND DISCUSSION

Figures 1 and 2 show imprinted hexagonal pillar arrays and line gratings, respectively, with periods of 500, 600, and 700 nm, alongside the silicon masters used as templates for the PDMS imprint molds. We find that up to approximately

TABLE I. Feature dimensions of imprinted TiO_2 and Si master molds in Figs. 1 and 2. Residual layer thickness refers to the thickness of the continuous film underneath the imprinted structures. Height refers to pillar height and groove depth, measured from the top interface of the residual layer. Volume refers to the pillar volume (nm^3) for pillars and the cross-sectional grating-ridge area (nm^2) for lines. Pillar volume is calculated with the model of a truncated cone; line volume is calculated with the model of a trapezoid. The height (volume) shrinkage factor $f_z(f)$ is defined as TiO_2 height /Si height (TiO_2 volume/Si volume).

Pattern/period (nm)	TiO_2 residual layer thickness (nm)	TiO_2 height (nm)	TiO_2 volume (nm^3/nm^2)	Si height (nm)	Si volume (nm^3/nm^2)	f_z	f
Pillars/500	85 ± 2	175 ± 2	$1.3 \pm 0.1 \times 10^6$	400 ± 3	$8.5 \pm 0.5 \times 10^6$	0.44	0.15
Pillars/600	82 ± 2	168 ± 2	$2.4 \pm 0.2 \times 10^6$	380 ± 3	$1.9 \pm 0.1 \times 10^7$	0.44	0.13
Pillars/700	100 ± 3	170 ± 5	$4.3 \pm 0.5 \times 10^6$	385 ± 3	$3.1 \pm 0.1 \times 10^7$	0.44	0.14
Lines/500	65 ± 3	90 ± 3	$1.2 \pm 0.2 \times 10^4$	370 ± 5	$1.0 \pm 0.1 \times 10^5$	0.24	0.12
Lines/600	30 ± 3	125 ± 5	$1.9 \pm 0.2 \times 10^4$	353 ± 5	$1.2 \pm 0.1 \times 10^5$	0.35	0.16
Lines/700	44 ± 4	105 ± 5	$2.0 \pm 0.2 \times 10^4$	353 ± 5	$1.4 \pm 0.1 \times 10^5$	0.30	0.14

80% of a total patterned area of 5.5 cm^2 is imprinted without visible defects, with exception of the 500 nm period line gratings, which show cracks running along the grating direction after annealing (Fig. 2). The remaining approximately 20% of the area shows incomplete pattern transfer (shallow grating depth and weak diffraction colors), which may be caused by inhomogeneous pressure distribution during the manual imprinting process. The defect area was not correlated with a certain pattern type or period. The pressure during the first 1 s of the imprinting process, during which the PDMS is pressed onto the precursor film, is approximately 0.02 MPa (3 psi). This low pressure avoids macroscopic distortion of the PDMS, and it is more than 20 times lower than the pressure of 5 atm (0.5 MPa or 73 psi) reported by Yoon *et al.*[16] Both solvent content and thickness of the spin-coated precursor film are identified as important parameters for obtaining high-quality imprints. If the solvent content is not sufficiently high, the precursor film material is not compliant enough for optimum pattern transfer. If the film is too thick, material shrinkage during annealing leads to film cracking and/or delaminating. Both solvent content and film thickness are controlled through TiO_2 precursor concentration, solvent type, maximum speed, and duration of spin coating. We find that a short spin coating step at high speed and a high precursor concentration, as detailed in Sec. II, give the best results. Another important parameter for obtaining high-quality imprint results is the compliance of the PDMS mold, with optimum results obtained from very soft PMDS that was cured for only 30 min, as described above. If PDMS was cured at higher temperature and for longer duration, the material was harder and a much higher pressure was needed to imprint a significant area; this, in turn, led to the distortion of grating patterns.

The side-view images (88° viewing angle) of the imprinted TiO_2 structures and corresponding Si master molds in Figs. 1 and 2, all of which are shown on the same scale, reveal a significant reduction in imprint feature sizes. Table I shows the results of a quantitative examination of the feature dimensions. Throughout this paper we characterize shrinkage in terms of shrinkage factors (the final height, width, or volume relative to the initial height, width, or volume), which makes the comparison of linear and volumetric shrinkage mathematically easier and more straightforward than with conventional definition for shrinkage. We were not able to image cross sections of the PDMS imprint molds with sufficient accuracy because of the softness of the material. We therefore cannot make an accurate assessment of the actual imprint mold dimensions but rather compare the annealed TiO_2 feature dimensions to those of the original Si master. For the discussion of constrained shrinkage, below, we assume that, before annealing, the TiO_2 precursor had filled a void in the PDMS mold equal in size to that of the Si features. This assumption will lead to an overestimation of the amount of shrinkage because it does not account for air trapped inside the PDMS mold. For the pillars, the height-shrinkage factor, as defined in the caption of Table I, is $f_z = 0.44$ for all three patterns. The corresponding volume-shrinkage factor is $f = 0.13 \pm 0.01$. For the lines, height shrinkage is more pronounced than for the pillars, $f_z = 0.30 \pm 0.05$. The corresponding volume-shrinkage factor is comparable to that of the pillars, $f = 0.16 \pm 0.04$. The similarity of the values for f is expected because f is a material specific not a shape-specific parameter.

The volumetric shrinkage of annealed sol-derived TiO_2 material is expected and further discussed below. We note, however, that the height-shrinkage factor for our pillar structures of 0.44 (equivalent to linear shrinkage of 56%) is less severe than that for a comparable precursor material reported by Yoon *et al.*, 0.32 (linear shrinkage of 68%).[16] We also note that the largest aspect ratio (height:width at 50% height) we observe is 2:1 and is found for the pillars in the 500 nm period array (Fig. 1).

We first discuss the role of substrate constraint on the observed shrinkage factors. In the case of (isotropic) volumetric shrinkage f, with f = final material volume/initial volume, the linear x, y, and z dimensions of a *freestanding* object shrink by a factor

$$f_x = f_y = f_z = f^{1/3}. \tag{1}$$

Here, f_x and f_y are defined similar to f_z in the caption of Table I. *Constrained* shrinkage, which has been studied for the case of sintering of ceramic particles both experimentally[21] and theoretically,[22] leads to changes in the linear dimensions that depend on both f and the object's geometry: for a film constrained by a substrate the lateral shrinkage is suppressed ($f_x = f_y = 1$) and the full shrinkage must be accommodated in the z dimension (perpendicular to film plane),

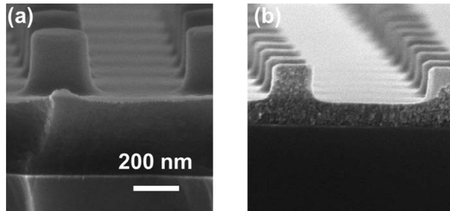

FIG. 3. SEM micrographs of nanoimprinted TiO_2 pillars after (a) 190 °C annealing and after (b) 500 °C annealing. (a) and (b) have the same magnification.

$$f_z = f. \tag{2}$$

For a partially constrained object, such as a pillar or a ridge, the height-shrinkage factor is expected to lie between

$$f^{1/3} > f_z > f, \tag{3}$$

and the lateral shrinkage factors follow

$$f_{x,y} > f^{1/3}. \tag{4}$$

Both the pillars in Fig. 1 and the ridges in Fig. 2 are partially constrained by the substrate. The observed values for f_z (Table I) indeed follow the expected trend: for an average volume-shrinkage factor (pillars and ridges) of $f = 0.14 \pm 0.2$, one obtains $f^{1/3} = 0.52 \pm 0.3$, and, for both pillars and lines, inequality (3) is satisfied. In addition, the height shrinkage for the lines is more pronounced than for the pillars, which is qualitatively expected because of the higher degree of substrate constraint of the lines, bringing f_z closer to the volume value f.

We also investigated constrained shrinkage without the previous assumptions regarding PDMS mold dimensions. We present here the results for a square pillar array that was annealed at 190 and 500 °C (see Fig. 3 and Table II). Annealing at 190 °C sufficiently stabilizes the imprinted features for SEM imaging while still not leading to full calcination (and shrinkage). From the residual layer thicknesses (Fig. 3 and Table II) and Eq. (2) we obtain $f = 0.30 \pm 0.05$ (and hence $f^{1/3} = 0.67 \pm 0.03$). The *directly measured* height-shrinkage factor, $f_z = 0.59 \pm 0.02$, satisfies inequality (3). The directly measured lateral shrinkage factor, obtained from the width at 50% height, is $f_{x,y} = 0.70 \pm 0.02$, which satisfies inequality (4). As a control we also calculate the volume shrinkage using the cone volumes, obtained by a model of a truncated cone, and we obtain the volume-shrinkage factor $f = 0.25 \pm 0.04$. This value is smaller but within the error margin of the value derived from the residual layer thickness.

TABLE II. Feature dimensions of imprinted TiO_2 pillars that are annealed at 190 and 500 °C.

Sample	Residual layer thickness (nm)	Height (nm)	Width at 50% height (nm)
(a) 190 °C anneal	320 ± 10	280 ± 3	255 ± 3
(b) 500 °C anneal	101 ± 2	165 ± 3	178 ± 2

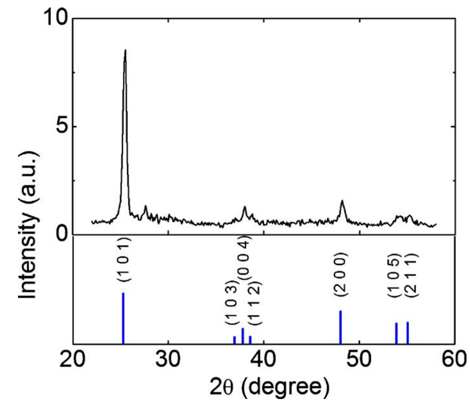

FIG. 4. (Color online) XRD scan of a 100-μm-thick annealed (500 °C) TiO_2 film on a Si (100) wafer. The strong Si (400) diffraction peak at $2\theta = 69.290°$ lies outside of the displayed data range. The bars indicating peak position and intensities are obtained from the PDF No. 021-1272 database for anatase TiO_2.

The volume shrinkage of sol-derived oxide films is mainly due to the removal of alkoxide groups and stabilizers. Our precursor solution contains 0.0198 mol Ti ions and 0.0100 mol H_2O molecules. Thus, only 1/8 of Ti-OBu bonds in the precursor are hydrolyzed, according to the reaction[23]

$$\mathrm{Ti(OBu)_4 + H_2O \rightarrow HO\text{-}Ti(OBu)_3 + BuOH}. \tag{5}$$

Both bound OBu groups, BuOH, amines, and solvent are present in the precursor solution during imprinting. Alcohol and possibly BuOH diffuse into the PDMS during the first annealing step. The results presented in Fig. 3 demonstrate that significant shrinkage takes place in the 500 °C annealing step.

Figure 4 shows data from a θ-2θ XRD scan for a film annealed at 500 °C. This result clearly shows that the crystalline structure of the material is anatase TiO_2, which is expected for the annealing temperature.[16,24,25]

The optical properties of the film material are important for photonic applications, as discussed above. Ellipsometry results presented in Fig. 5 show that the film absorption is very low and that the average index of refraction in the

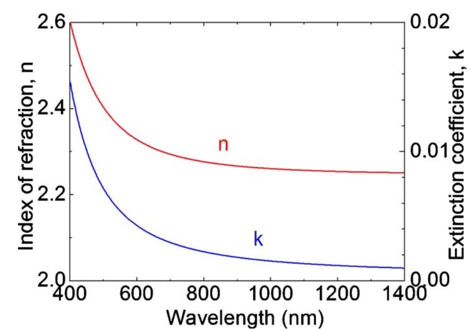

FIG. 5. (Color online) Optical constants n and k for a 95-μm-thick annealed (500 °C) TiO_2 film on a Si (100) wafer, obtained from ellipsometry. The n values are fitted to a Cauchy model with the parameters $A = 2.245$, $B = 0.007\,99$, and $C = 0.007\,92$. k is fitted to an exponential model. The mean square error for the fit of the combined n, k model is 13.948, which is considered a good fit of the experimental data.

wavelength range of 800–1100 nm, important for light-trapping applications for crystal silicon photovoltaics, is $n = 2.27 \pm 0.01$. The index is lower than the corresponding anatase bulk material, which has the index $n = 2.488 - 2.561$ at 589 nm wavelength (depending on crystallographic orientation).[26] Our film has an index of $n = 2.33$ at 589 nm wavelength, which is approximately 8% lower than the average bulk value. The lower index is commonly explained by voids in the material filled with air and/or solvent.[27]

IV. CONCLUSIONS

We report a soft-imprint method for obtaining anatase TiO_2 nanostructures using a sol-based precursor film. The method employs of a very low imprint pressure of 0.02 MPa (3 psi), which is easily applied by hand, without dedicated imprint equipment. The use of a heavy alcohol as precursor solvent, a very brief spin coating time, and the use of an incompletely cross-linked PDMS mold are all found to be crucial for obtaining high-quality imprint results. The height-shrinkage factor (TiO_2 feature height/Si master height) for pillars is only 0.44, which is a smaller degree of shrinkage than reported in the literature (factor 0.32) for a comparable chemistry. Constrained volumetric shrinkage is discussed for both pillar arrays and line gratings. The design dimensions of a master imprint mold will have to take shrinkage into account. We believe that this method is transferable to other metal alkoxide-based sol chemistries.

ACKNOWLEDGMENTS

This work was supported by the U.S. Department of Energy with a Photovoltaic Supply Chain and Cross-Cutting Technologies Grant No. DE-EE0000586. Fabrication and microscopy were performed at the Washington Technology Center Microfabrication Laboratory and the University of Washington Nanotech User Facility, members of the NSF National Nanotechnology Infrastructure Network. Paul Wallace's help with PDMS processing and ellipsometry and Wei Zhang's help with x-ray diffraction are gratefully acknowledged (both in University of Washington). D.N.W. acknowledges helpful discussions on constrained sintering with Rajendra K. Bordia (University of Washington).

[1]W. Lukosz and K. Tiefenthaler, Opt. Lett. **8**, 537 (1983).
[2]K. Heuberger and W. Lukosz, Appl. Opt. **25**, 1499 (1986).
[3]R. Brendel, A. Gier, M. Mennig, H. Schmidt, and J. H. Werner, J. Non-Cryst. Solids **218**, 391 (1997).
[4]C. Marzolin, S. P. Smith, M. Prentiss, and G. M. Whitesides, Adv. Mater. **10**, 571 (1998).
[5]S. Seraji, Y. Wu, N. E. Jewell-Larson, M. J. Forbess, S. J. Limmer, T. P. Chou, and G. Z. Cao, Adv. Mater. **12**, 1421 (2000).
[6]A. Gombert, W. Glaubitt, K. Rose, J. Dreibholz, B. Blasi, A. Heinzel, D. Sporn, W. Döll, and V. Wittwer, Sol. Energy **68**, 357 (2000).
[7]M. T. Li, H. Tan, L. Chen, J. Wang, and S. Y. Chou, J. Vac. Sci. Technol. B **21**, 660 (2003).
[8]S. Matsui, Y. Igaku, H. Ishigaki, J. Fujita, M. Ishida, Y. Ochiai, H. Namatsu, and M. Komuro, J. Vac. Sci. Technol. B **21**, 688 (2003).
[9]C. Harnagea, M. Alexe, J. Schilling, J. Choi, R. B. Wehrspohn, D. Hesse, and U. Gösele, Appl. Phys. Lett. **83**, 1827 (2003).
[10]V. C. Sundar, H. J. Eisler, T. Deng, Y. T. Chan, E. L. Thomas, and M. G. Bawendi, Adv. Mater. **16**, 2137 (2004).
[11]C. Goh, K. M. Coakley, and M. D. McGehee, Nano Lett. **5**, 1545 (2005).
[12]S. Z. Chen, J. F. Liu, H. J. H. Chen, and F. S. Huang, J. Vac. Sci. Technol. B **24**, 1934 (2006).
[13]C. Peroz, C. Heitz, E. Barthel, E. Søndergård, and V. Goletto, J. Vac. Sci. Technol. B **25**, L27 (2007).
[14]C. Peroz, V. Chauveau, E. Barthel, and E. Søndergård, Adv. Mater. **21**, 555 (2009).
[15]J. Kim, M. Kim, M. J. Lee, J. S. Lee, K. Shin, and Y. S. Kim, Adv. Mater. **21**, 4050 (2009).
[16]K. M. Yoon, K. Y. Yang, and H. Lee, Thin Solid Films **518**, 126 (2009).
[17]R. Ji, M. Hornung, M. A. Verschuuren, R. van de Laar, J. van Eekelen, U. Plachetka, M. Moeller, and C. Moormann, Microelectron. Eng. **87**, 963 (2010).
[18]D. N. Weiss, S. T. Meyers, and D. A. Keszler, J. Vac. Sci. Technol. B **28**, 823 (2010).
[19]D. N. Weiss, H.-C. Yuan, B. G. Lee, H. M. Branz, S. T. Meyers, A. Grenville, and D. A. Keszler, J. Vac. Sci. Technol. B **28**, C6M98 (2010).
[20]Y. N. Xia and G. M. Whitesides, Annu. Rev. Mater. Sci. **28**, 153 (1998).
[21]O. Guillon, E. Aulbach, J. Rödel, and R. K. Bordia, J. Am. Ceram. Soc. **90**, 1733 (2007).
[22]C. L. Martin and R. K. Bordia, Acta Mater. **57**, 549 (2009).
[23]C. J. Brinker and G. W. Scherer, *Sol-Gel Science: The Physics and Chemistry of Sol-Gel Processing* (Academic, San Diego, 1990), pp. 2–11.
[24]H. D. Nam, B. H. Lee, S. J. Kim, C. H. Jung, J. H. Lee, and S. Park, Jpn. J. Appl. Phys., Part 1 **37**, 4603 (1998).
[25]D. Regonini, A. Jaroenworaluck, R. Stevens, and C. R. Bowen, Surf. Interface Anal. **42**, 139 (2010).
[26]*CRC Handbook of Chemistry and Physics*, 81st ed., edited by D. R. Lide (CRC, Boca Raton, 2000), pp. 4–141.
[27]K. Jiang, A. Zakutayev, J. Stowers, M. D. Anderson, J. Tate, D. H. McIntyre, D. C. Johnson, and D. A. Keszler, Solid State Sci. **11**, 1692 (2009).